Cell Genomics, Volume *3*

Supplemental information

Transposable elements are associated with the variable response to influenza infection

Xun Chen, Alain Pacis, Katherine A. Aracena, Saideep Gona, Tony Kwan, Cristian Groza, Yen Lung Lin, Renata Sindeaux, Vania Yotova, Albena Pramatarova, Marie-Michelle Simon, Tomi Pastinen, Luis B. Barreiro, and Guillaume Bourque

SUPPLEMENTARY FIGURES

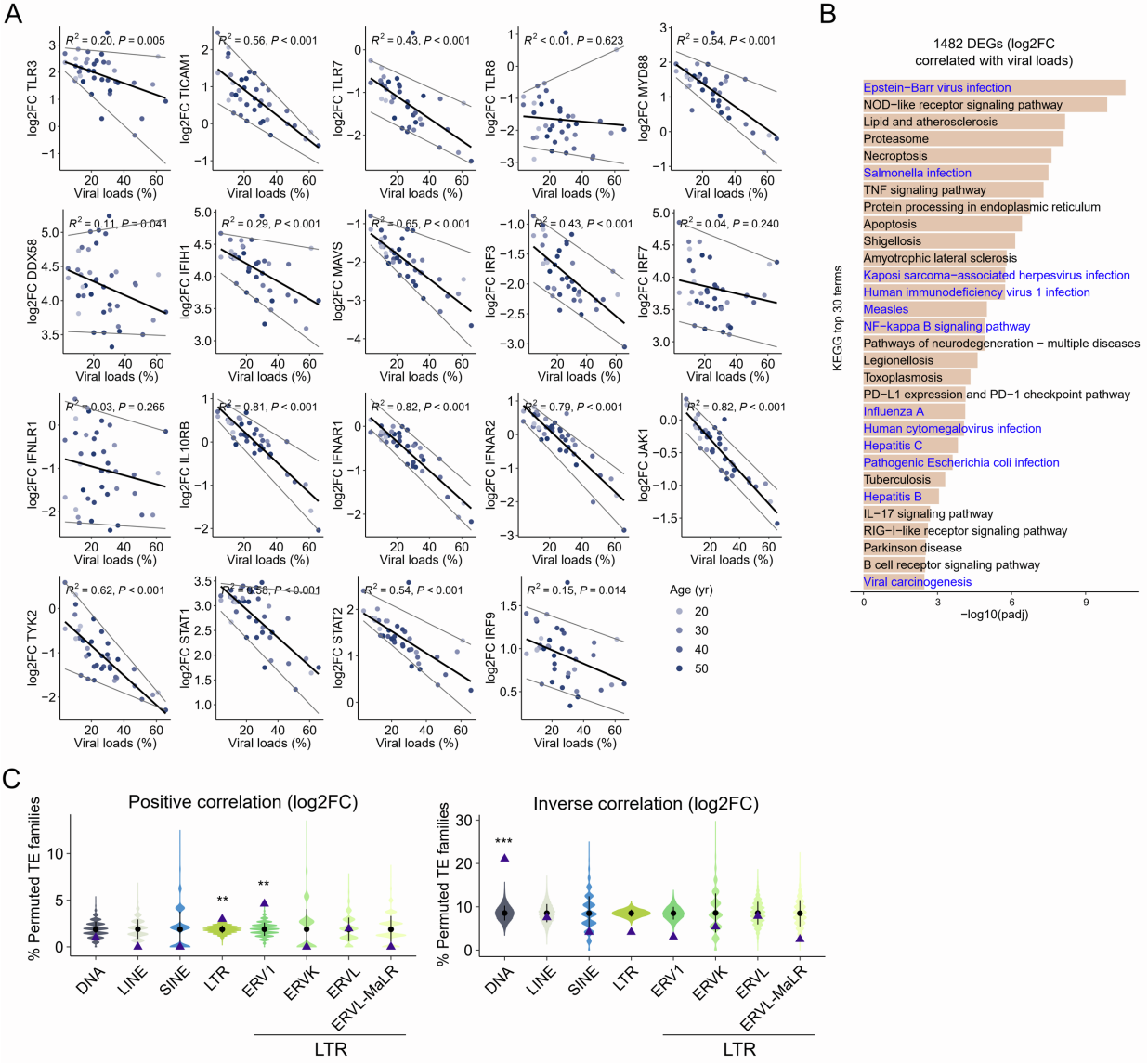

Figure S1. Immune genes and few TE families are prone to correlate with viral load post-infection, related to Figure 1

(A) Expression fold changes (log2FCs) of most key immune regulators are inversely correlated with viral load post-infection. Many genes are shown to strongly correlate with viral load, including membrane-bound receptor genes sensing infection-induced interferons, *i.e.*, *IL10RB*, *IFNAR1*, *IFNAR2*, and *JAK1*. Linear regression model was used for the correlation analysis.

Black line represents the regression line and grey lines represent the 5% and 95% quantiles. **(B)** Expression fold change amongst differentially expressed genes (DEGs) correlated with viral load are enriched in multiple virus infection pathways. 1,482 DEGs with log2FCs correlated with viral load ($R^2 \geq 0.3$, p value ≤ 0.05) were identified and used for downstream pathway enrichment analysis. **(C)** Enrichment of the proportion for log2FC amongst TE families positively and inversely correlated with viral load post-infection. 17 positively and 77 inversely correlated TE families were analyzed. Purple triangle represents the actual proportion of correlated families among subclass or superfamily. Error bar represents the mean values and standard deviations of 10,000 randomized proportions. One-tailed student's *t*-test was used to compare the actual proportions with randomized proportions (* $p \leq 0.05$, ** $p \leq 0.01$, *** $p \leq 0.001$).

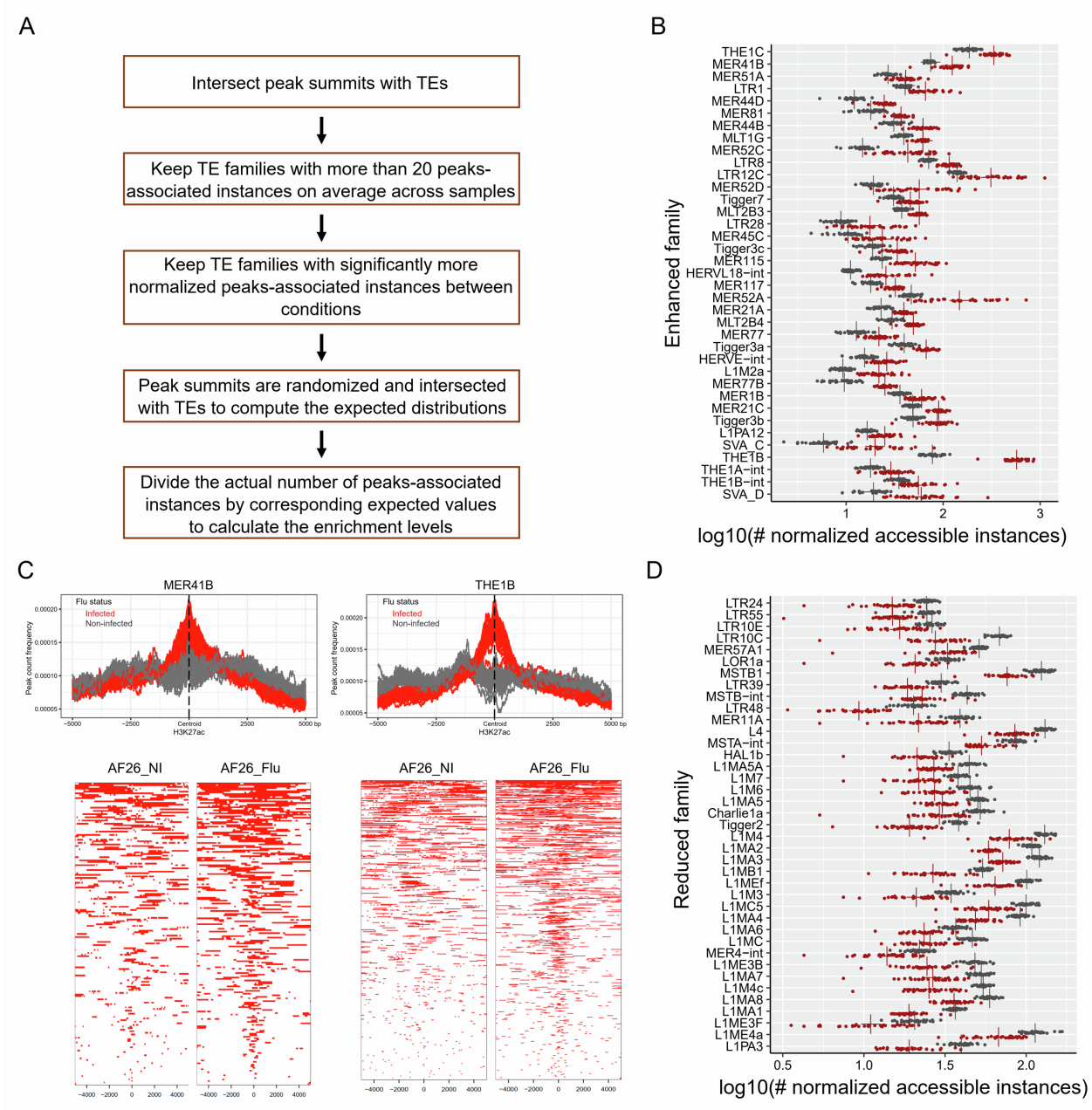

Figure S2. Detection of TE families with enhanced and reduced accessibility in response to IAV infection, related to Figure 2

(A) Optimized TE enrichment analysis pipeline. Details were described in Methods. **(B)** Distributions of the normalized number of peaks-associated instances of TE families with enhanced accessibility. Each point represents one sample. Grey color represents the non-infected

sample and red color represents the infected sample. "+" indicates the mean value across non-infected (grey) and infected (red) samples. The number of accessible instances were normalized by the average number of peaks across infected and non-infected samples, respectively. **(C)** Average profiles (up) and heatmaps (bottom) of H3K27ac peaks at MER41B and THE1B (± 5 kb). H3K27ac peaks are centered at the median positions of peak summits across infected samples. Peak regions are shown as heatmaps at the bottom. AF26 non-infected and infected samples are shown as examples. Peak regions centered at each family are shown as red bars. **(D)** Distributions of the normalized number of peaks-associated instances of TE families with reduced accessibility. Each point represents one non-infected (grey) and infected (red) sample. "+" indicates the mean value across non-infected (grey) and infected (red) samples. The number of accessible instances were normalized by the average number of peaks across infected and non-infected samples separately.

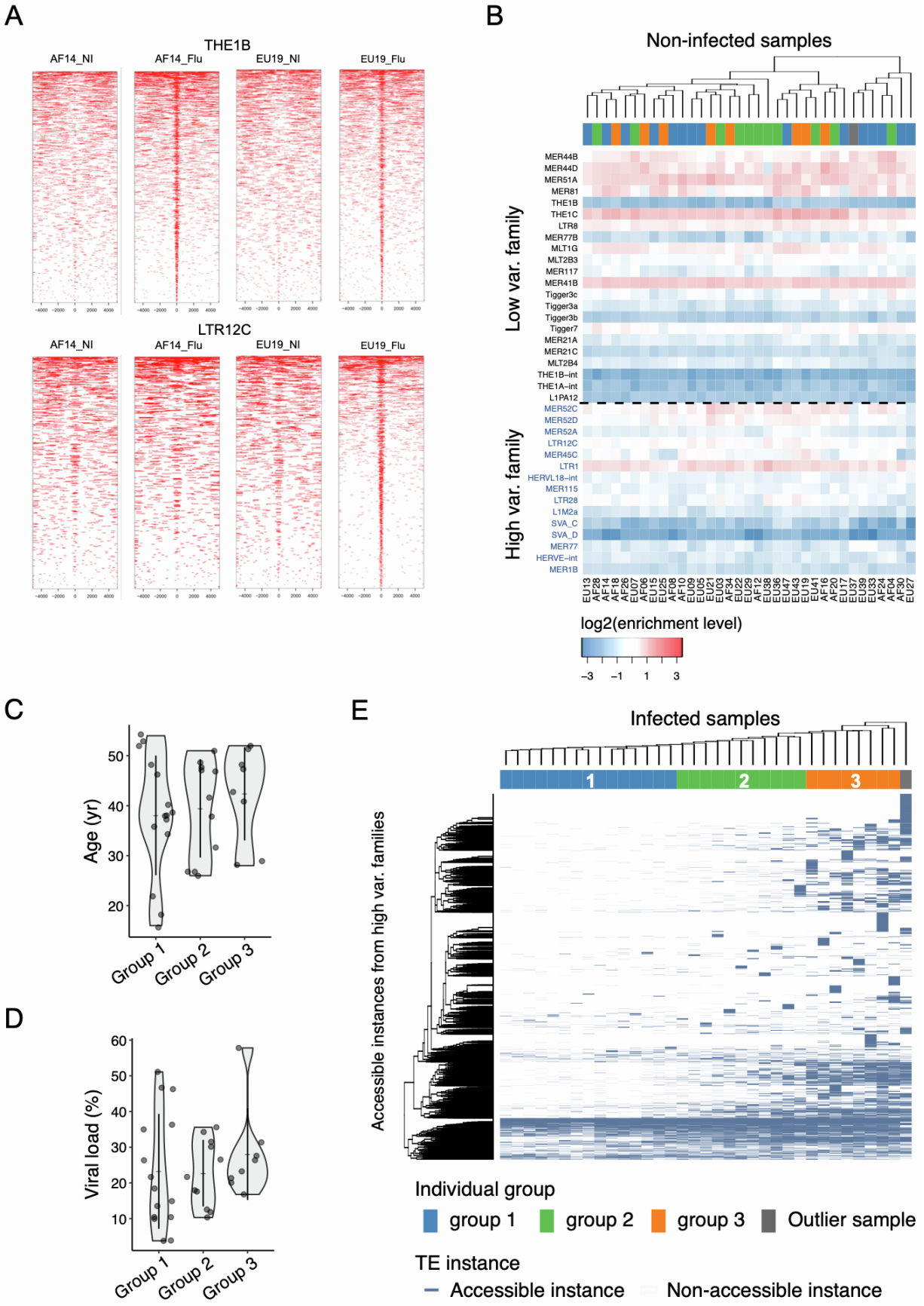
A
THE1B
AF14_NI
AF14_Flu
EU19_NI
EU19_Flu
LTR12C
AF14_NI
AF14_Flu
EU19_NI
EU19_Flu
B
Non-infected samples
Low var. family
High var. family
MER44B
MER44D
MER51A
MER81
THE1B
THE1C
LTR8
MER77B
MLT1G
MLT2B3
MER117
MER41B
Tigger3c
Tigger3a
Tigger3b
Tigger7
MER21A
MER21C
MLT2B4
THE1B–int
THE1A–int
L1PA12
MER52C
MER52D
MER52A
LTR12C
MER45C
LTR1
HERVL18–int
MER115
LTR28
L1M2a
SVA_C
SVA_D
MER77
HERVE–int
MER1B
log2(enrichment level)
–3
–1
1
3
C
Age (yr)
50
40
30
20
Group 1
Group 2
Group 3
D
Viral load (%)
60
50
40
30
20
10
Group 1
Group 2
Group 3
E
Infected samples
1
2
3
Accessible instances from high var. families
Individual group
group 1
group 2
group 3
Outlier sample
TE instance
Accessible instance
Non-accessible instance

Figure S3. High variable families display high variability in chromatin accessibility post-infection, related to Figure 3

(A) Heatmaps of open chromatin regions at THE1B and LTR12C (± 5 kb). Two infected and non-infected samples are shown as examples. LTR12C shows a high variability of accessibility between randomly-selected samples post-infection. ATAC-seq peaks are centered at the summits in TEs. 5 kb upstream and downstream regions are shown. Compared to AF14, EU19 displays a higher enrichment at LTR12C but comparable enrichment at THE1B. **(B)** Heatmap of log2 enrichment levels of 37 enhanced families in 35 non-infected samples. Semi-clustering analysis was performed. Three individual groups observed at infected samples are not clustered together. High variable families are highlighted in blue color. **(C,D)** Violin plots of age of macrophage donors and viral load of the three individual groups. Group 3 individuals have relatively older ages and higher viral load compared to group 1 individuals. The dot represents each individual and the error bar represents the mean value and standard deviation. **(E)** Heatmap of the chromatin state of accessible instances from high variable families in 35 infected samples. The state of open chromatin is in blue color and closed chromatin in white color. Unsupervised clustering analysis was performed, and the three individual groups are clustered together. A fraction of instances shows an enrichment in group 3 compared to group 1 individuals.

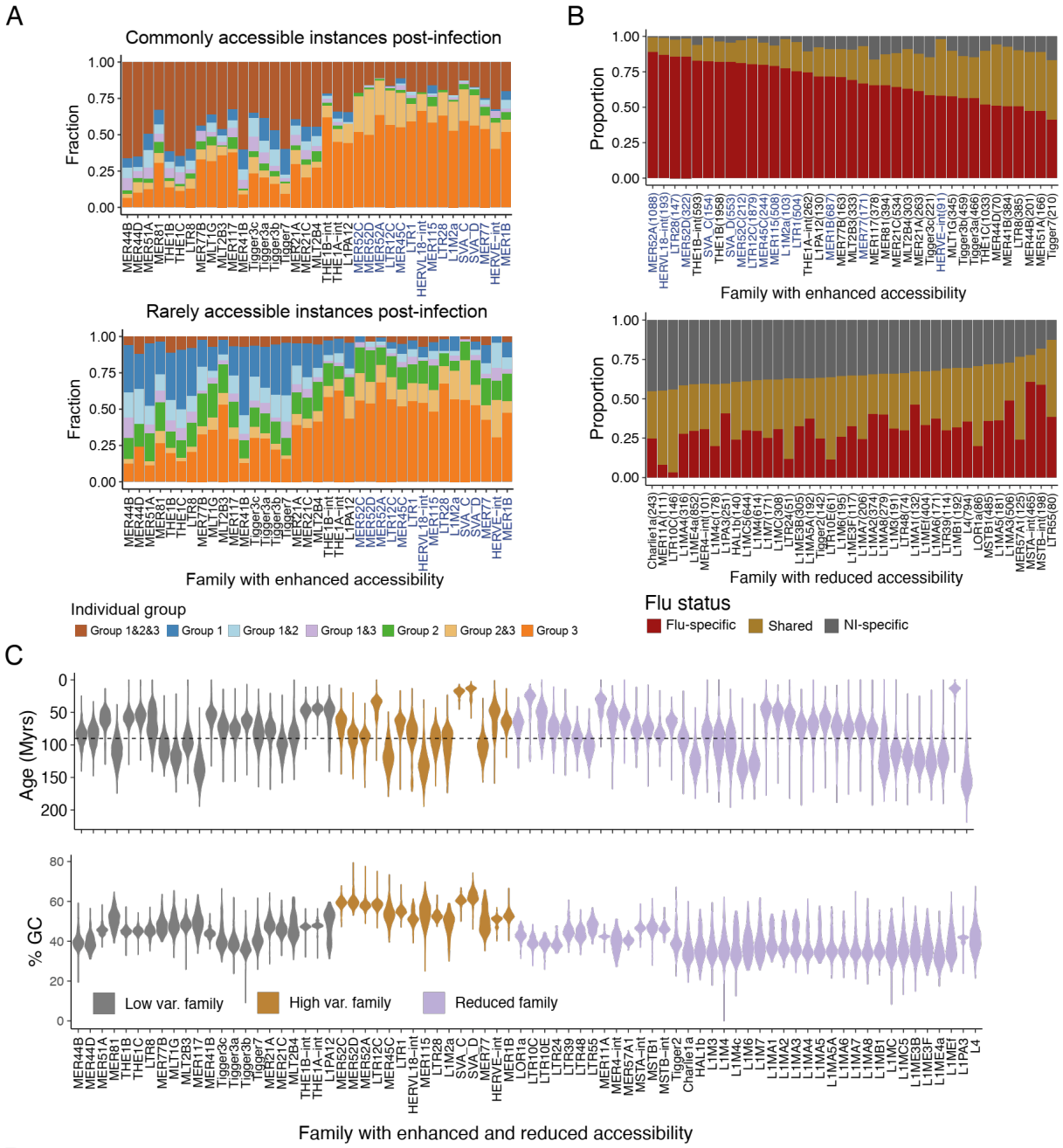
A
Commonly accessible instances post-infection
Fraction
Rarely accessible instances post-infection
Fraction
Family with enhanced accessibility
B
Proportion
Family with enhanced accessibility
Proportion
Family with reduced accessibility
Individual group
Group 1&2&3
Group 1
Group 1&2
Group 1&3
Group 2
Group 2&3
Group 3
Flu status
Flu-specific
Shared
NI-specific
C
Age (Myrs)
% GC
Low var. family
High var. family
Reduced family
Family with enhanced and reduced accessibility
D
log10(# instances in the human genome)
0.0003
Low var. families
High var. families
accessible instances
0.81
Low var. families
High var. families

Figure S4. Characteristics of TE families display high variability in chromatin accessibility post-infection, related to Figure 3

(A) Proportions of accessible instances per enhanced family are variable between three individual groups post infection. Commonly accessible instances represent instances that are accessible in more than 25% samples from at least one group (left); rarely accessible instances represent instances that are accessible in less than 25% samples from any groups (right). Enrichment in one individual group refers to instances that are accessible in more than 25% samples for commonly accessible instances and one or more samples for rarely accessible instances. High variable families are highlighted in blue color. **(B)** Proportions of flu-specific, shared, and NI-specific instances of each family with enhanced and reduced accessibility. Flu-specific instances represent instances that are accessible in ≥ 1 infected and no non-infected sample; NI-specific instances represent instances that are accessible in ≥ 1 non-infected and no infected sample; Shared instances represent instances that are accessible in ≥ 1 non-infected and ≥ 1 infected samples. High variable families are in blue color. **(C)** Violin plot of the estimated TE evolutionary ages (up) and GC contents (bottom). Dotted lines indicate the evolution time when primates diverged from other mammals (~90 million years ago). No distinct patterns are observed between high variable, low variable families, and reduced families. The estimation of ages was described in Methods. High variable families show a higher GC content compared to others. Group 3 individuals have comparable or lower GC content than other individuals, supporting that the higher accessibility in high variable families for group 3 individuals are not derived from sequencing artifacts. **(D)** Number of instances and accessible instances from high variable and low variable families. *P* values computed by two-tailed student's *t*-test are shown above the dot plots.

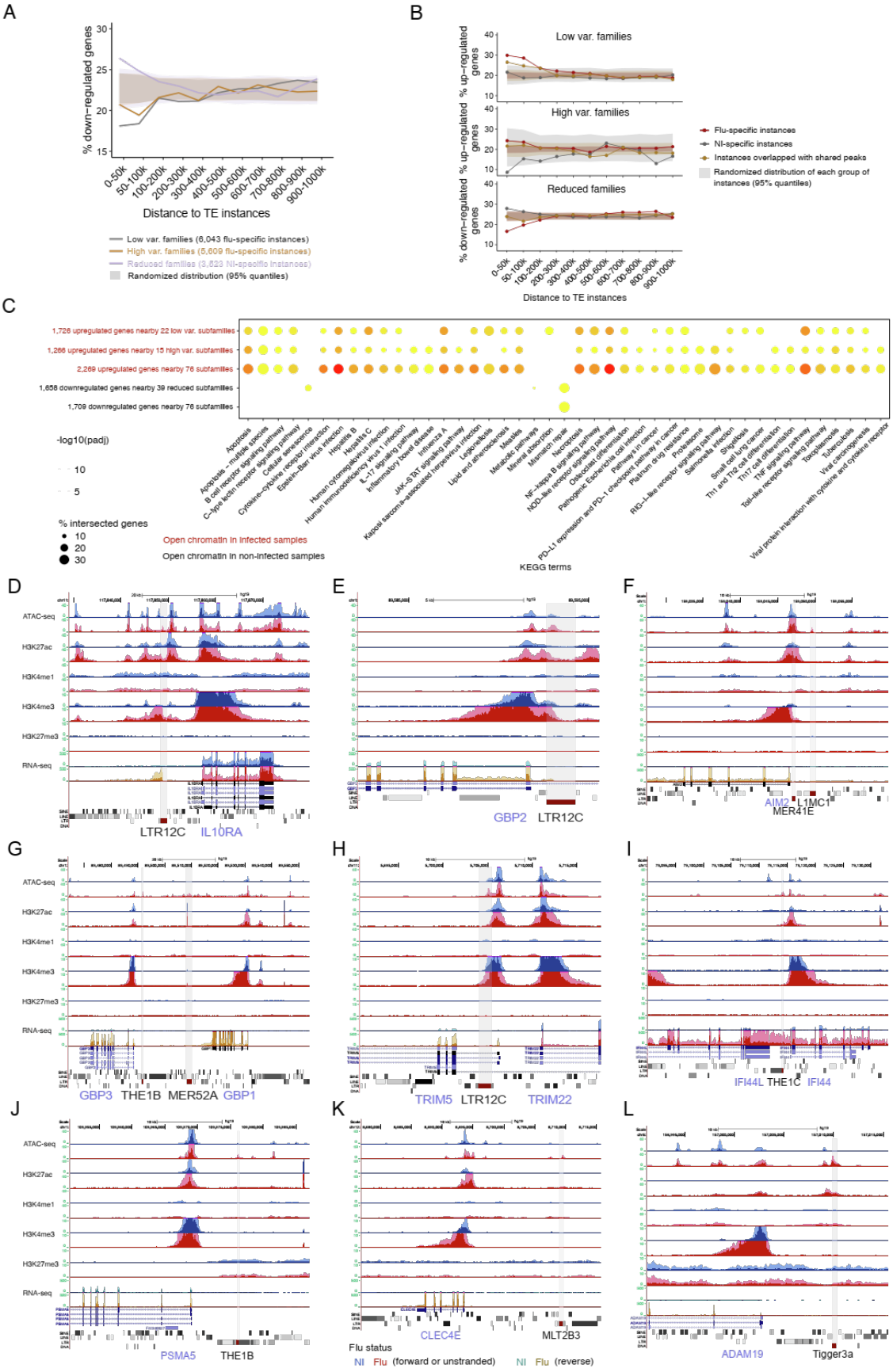
A
% down−regulated genes
Distance to TE instances
0-50k
50-100k
100-200k
200-300k
300-400k
400-500k
500-600k
600-700k
700-800k
800-900k
900-1000k
Low var. families (6,043 flu-specific instances)
High var. families (5,609 flu-specific instances)
Reduced families (3,823 NI-specific instances)
Randomized distribution (95% quantiles)
B
Low var. families
High var. families
Reduced families
% up−regulated genes
% down−regulated genes
Distance to TE instances
Flu-specific instances
NI-specific instances
Instances overlapped with shared peaks
Randomized distribution of each group of instances (95% quantiles)
C
1,726 upregulated genes nearby 22 low var. subfamilies
1,286 upregulated genes nearby 15 high var. subfamilies
2,269 upregulated genes nearby 76 subfamilies
1,658 downregulated genes nearby 39 reduced subfamilies
1,709 downregulated genes nearby 76 subfamilies
-log10(padj)
10
5
% intersected genes
10
20
30
Open chromatin in infected samples
Open chromatin in non-infected samples
Apoptosis
Apoptosis − multiple species
B cell receptor signaling pathway
C−type lectin receptor signaling pathway
Cellular senescence
Cytokine−cytokine receptor interaction
Epstein−Barr virus infection
Hepatitis B
Hepatitis C
Human cytomegalovirus infection
Human immunodeficiency virus 1 infection
IL−17 signaling pathway
Inflammatory bowel disease
Influenza A
JAK−STAT signaling pathway
Kaposi sarcoma−associated herpesvirus infection
Legionellosis
Lipid and atherosclerosis
Measles
Metabolic pathways
Mineral absorption
Mismatch repair
Necroptosis
NF−kappa B signaling pathway
NOD−like receptor signaling pathway
Osteoclast differentiation
Pathogenic Escherichia coli infection
Pathways in cancer
PD−L1 expression and PD−1 checkpoint pathway in cancer
Platinum drug resistance
Proteasome
RIG−I−like receptor signaling pathway
Salmonella infection
Shigellosis
Small cell lung cancer
Th1 and Th2 cell differentiation
Th17 cell differentiation
TNF signaling pathway
Toll−like receptor signaling pathway
Tuberculosis
Viral carcinogenesis
Viral protein interaction with cytokine and cytokine receptor
KEGG terms
D
E
F
ATAC-seq
H3K27ac
H3K4me1
H3K4me3
H3K27me3
RNA-seq
LTR12C
IL10RA
GBP2
LTR12C
AIM2
L1MC1
MER41E
G
H
I
GBP3
THE1B
MER52A
GBP1
TRIM5
LTR12C
TRIM22
IFI44L
THE1C
IFI44
J
K
L
PSMA5
THE1B
CLEC4E
MLT2B3
ADAM19
Tigger3a
Flu status
NI Flu (forward or unstranded)
NI Flu (reverse)

Figure S5. TE families with accessibility changes may co-opt in the immune response to IAV infection, related to Figure 4

(A) Fractions of down-regulated genes near accessible TEs relative to the random distributions. Proportions of down-regulated genes are shown within each of the genomic intervals relative to nearby accessible TEs. More details were described in **Figure 4A**. **(B)** Proportions of up/down-regulated genes near flu-specific, NI-specific, and shared instances. Proportions were computed within each of the genomic intervals relative to nearby accessible instances. Upregulated genes were analyzed for high variable and low variable families, and downregulated genes were analyzed for reduced families. Expected distributions were computed as we described in Methods (shaded regions, 95% confidence intervals). The proportions were compared with corresponding expected distributions. Flu-specific instances from low variable and high variable families and NI-specific instances from reduced families display the highest proportions of up/down-regulated genes within 100 kb relative to nearby accessible instances, particularly within 50 kb. **(C)** Pathway enrichment analysis of DEGs adjacent (≤ 50 kb) to each category of families. It shows the enrichment of multiple immune-related pathways near families with enhanced accessibility. Some pathways are differentially enriched between high variable and low variable families, including RIG-I-like receptor signaling pathway. **(D)** Genomic view of an accessible LTR12C with the expression was upregulated and initiated at the open chromatin region post-infection. The LTR12C instance highlighted as the shaded area shows an upregulated accessibility, expression, and H3K4me3 activity. *IL10RA* gene located near the LTR12C instance is also significantly upregulated post-infection. **(E-L)** Example genomic views of instances with enhanced accessibility post-infection. Instances are highlighted as the shaded areas. Eight TE immune-related gene pairs are shown, i.e., LTR12C-*GBP2*, MER41-*AIM2*, MER52A/THE1B-

GBP1/3, LTR12C-*TRIM22*, THE1C-*IFI44*, THE1B-*PSMA5*, and MLT2B3-*CLEC4E*, and Tigger3a-*ADAM19*. *GBP2* has been validated to be regulated by the upstream LTR12C instance.[1] *AIM2* has also been validated to be regulated by a MER41 instance;[2] interestingly, it may also be regulated by another TE instance. Other three TE instances reported by Chuong et al.[2] that potentially regulate *APOL1*, *IFI6*, and *SECTM1* did not show chromatin change in macrophages (https://computationalgenomics.ca/tools/epivar). The dark shaded area denotes the distribution of the average RPM values and the light shaded area denotes the standard deviation. Signals of various epigenetic marks are shown in blue color for non-infected samples and red color for infected samples. For RNA-seq, forward and reverse transcripts are shown in blue and green color separately for non-infected samples; while forward and reverse transcripts are shown in red and brown color separately for infected samples.

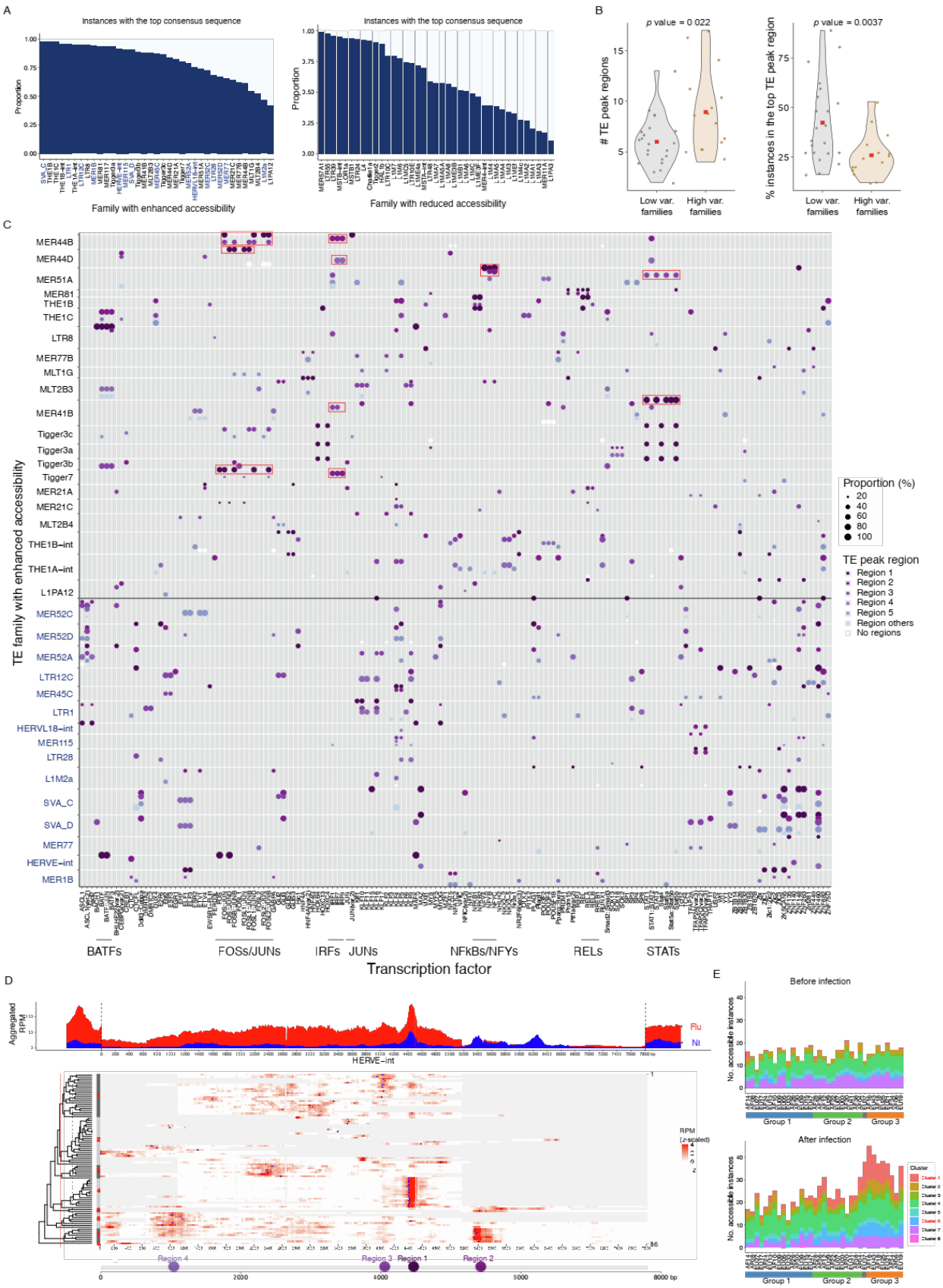
A
Instances with the top consensus sequence
Proportion
Family with enhanced accessibility
Instances with the top consensus sequence
Proportion
Family with reduced accessibility
B
p value = 0.022
TE peak regions
Low var. families
High var. families
p value = 0.0037
% instances in the top TE peak region
Low var. families
High var. families
C
TE family with enhanced accessibility
MER44B
MER44D
MER51A
MER81
THE1B
THE1C
LTR8
MER77B
MLT1G
MLT2B3
MER41B
Tigger3c
Tigger3a
Tigger3b
Tigger7
MER21A
MER21C
MLT2B4
THE1B–int
THE1A–int
L1PA12
MER52C
MER52D
MER52A
LTR12C
MER45C
LTR1
HERVL18–int
MER115
LTR28
L1M2a
SVA_C
SVA_D
MER77
HERVE–int
MER1B
BATFs
FOSs/JUNs
IRFs
JUNs
NFkBs/NFYs
RELs
STATs
Transcription factor
Proportion (%)
20
40
60
80
100
TE peak region
Region 1
Region 2
Region 3
Region 4
Region 5
Region others
No regions
D
Aggregated RPM
HERVE–int
Flu
NI
RPM [z-scaled]
Region 4
Region 3
Region 1
Region 2
E
Before infection
No. accessible instances
Group 1
Group 2
Group 3
After infection
No. accessible instances
Cluster
Group 1
Group 2
Group 3

Figure S6. TE peak regions and TF binding motifs reveal the association of high variability in chromatin accessibility with KRAB-ZNFs, related to Figure 5

(A) Proportions of accessible instances with top candidate consensus sequences. Consensus sequence information was achieved from the ".align" files generated by RepeatMasker. It shows a high proportion for TE families with enhanced accessibility. High variable families are highlighted in blue color. **(B)** Number of TE peak regions detected for high variable and low variable families. Compared to low variable families, high variable families have significantly more TE peak regions and more instances in the top TE peak region. *P* values were computed by the two-tailed student's *t*-test. **(C)** TF binding motifs enriched in each TE peak region of families with enhanced accessibility. Top five TE peak regions are shown. Instances in other regions and instances not within TE peak regions were analyzed separately. TE peak regions of each family are shown as separate rows. Dot size refers to the proportion of instances in each region containing each motif. Dotted line separates high variable and low variable families and high variable families are also highlighted in blue color. **(D)** Aggregated RPM (up) and RPM (bottom) values on each instance along the HERVE-int consensus sequence. Infected (red) and non-infected (blue) samples are shown separately including the upstream and downstream regions (± 20% of the consensus sequence length). Computed RPM values were *z*-scaled in the heatmap while values below zero are in white color. Deletions relative to the consensus sequence are shown in grey color. Unsupervised clustering analysis was performed with the scaled RPM values to determine the main clusters. Blue triangles indicate the peak centroids referring to the highest RPM values. TE peak regions and positions are shown in the bottom (Same as **Figure 5B**). More details were described in Methods. **(E)** Number of accessible instances from each cluster. Infected and non-infected samples are shown separately. Individuals are ordered based

on the clustering obtained in **Figure 3C**. Instances from Cluster 1 and 6, most of which contain TE peak region 3 and 4, are more abundant in group 3 individuals than group 1 individuals.

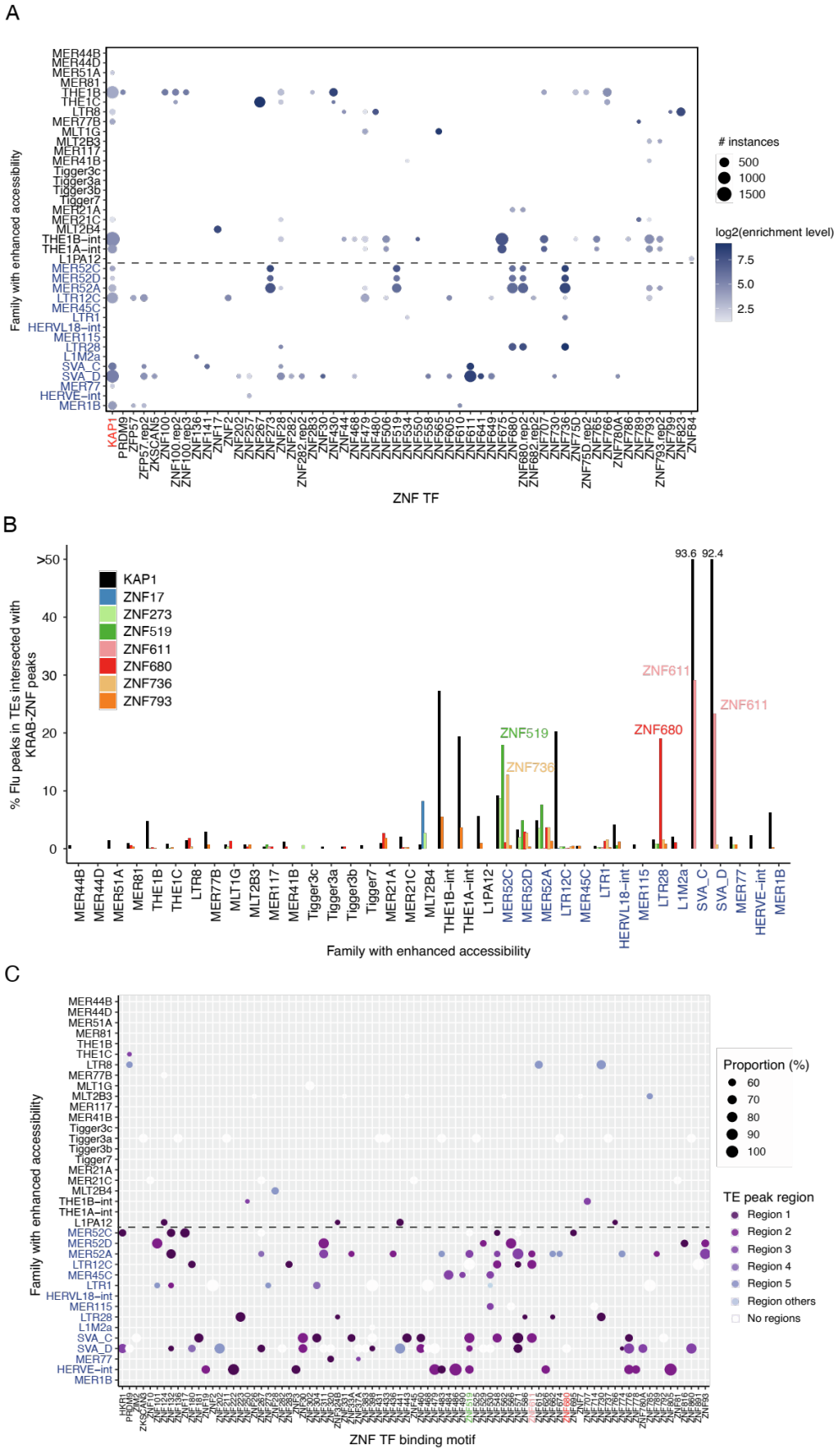
A
Family with enhanced accessibility
ZNF TF
instances
500
1000
1500
log2(enrichment level)
7.5
5.0
2.5
B
% Flu peaks in TEs intersected with KRAB-ZNF peaks
Family with enhanced accessibility
KAP1
ZNF17
ZNF273
ZNF519
ZNF611
ZNF680
ZNF736
ZNF793
93.6
92.4
ZNF611
ZNF611
ZNF680
ZNF519
ZNF736
C
Family with enhanced accessibility
ZNF TF binding motif
Proportion (%)
60
70
80
90
100
TE peak region
Region 1
Region 2
Region 3
Region 4
Region 5
Region others
No regions

Figure S7. KAP1 and KRAB-ZNFs are associated with high variability in chromatin accessibility in high variable families, related to Figure 5

(A) Enrichment levels of KRAB-ZNF binding sites in high variable and low variable families in 257 HEK293T cell lines.[3] High variable families like MER52s, SVAs, LTR12C, and LTR28 are shown to be enriched for KRAB-ZNF binding sites. Color intensity refers to the fold enrichment relative to the random distribution (see Methods). (**B**) Proportion of KAP1 and KRAB-ZNF binding sites that overlap with accessible regions in TEs post-infection. A 100-bp of genomic region centered at the ATAC-seq peak centroids was used for this analysis. KRAB-ZNFs with a minimum of 5% across enhanced families were visualized. **(C)** KRAB-ZNF binding motifs enriched in enhanced families. Motifs were obtained from Barazandeh et al.[4] Same motifs enriched across TE peak regions are aggregated. TE peak regions with the most instances are shown as representatives. KRAB-ZNFs with their enrichment of binding sites in high variable families are highlighted.

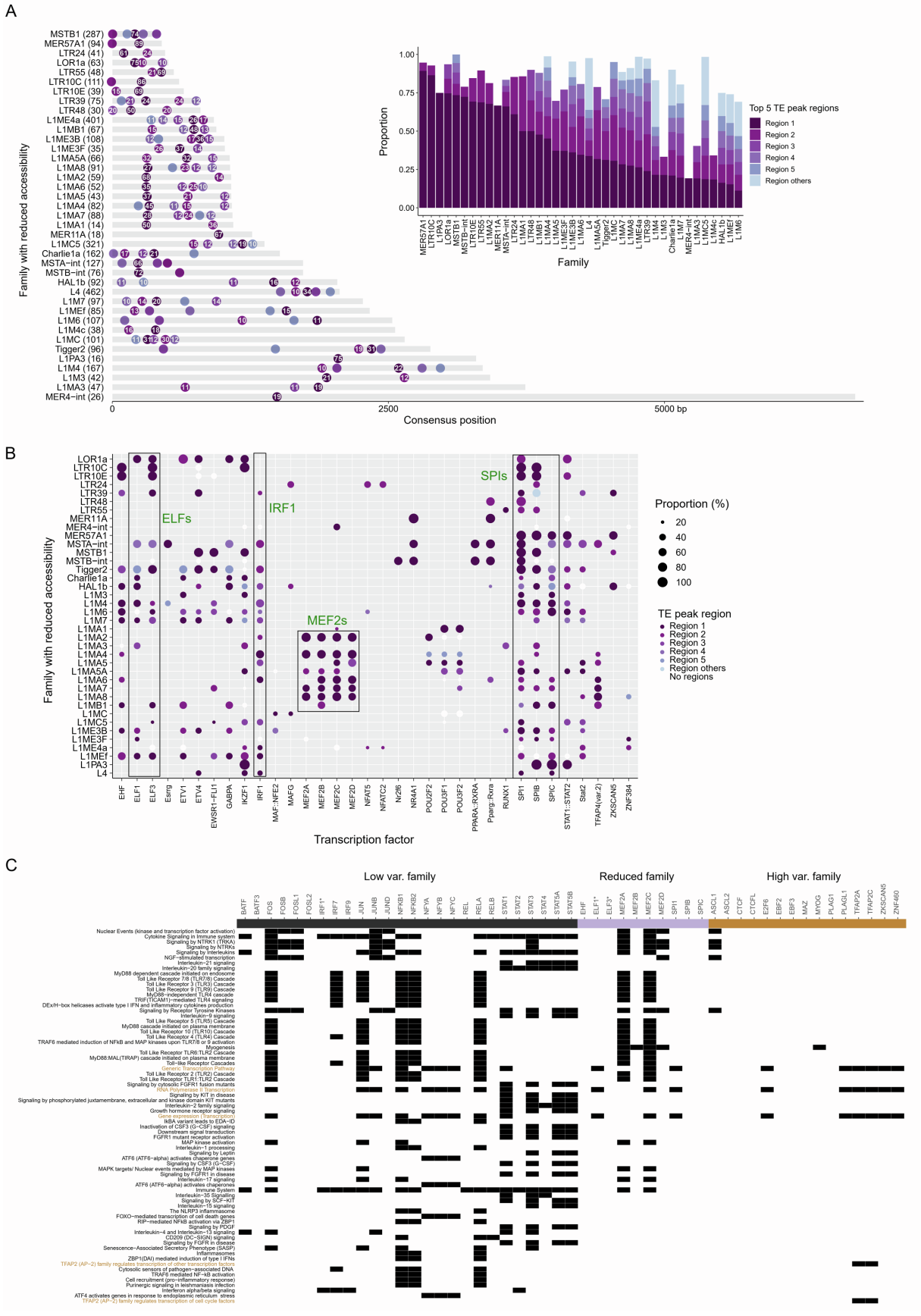
A
Family with reduced accessibility
Consensus position
0
2500
5000 bp
Proportion
Family
Top 5 TE peak regions
Region 1
Region 2
Region 3
Region 4
Region 5
Region others
B
Family with reduced accessibility
Transcription factor
ELFs
IRF1
MEF2s
SPIs
Proportion (%)
TE peak region
Region 1
Region 2
Region 3
Region 4
Region 5
Region others
No regions
C
Low var. family
Reduced family
High var. family

Figure S8. TE Peak regions and TF binding motifs enriched in reduced families and different sets of TE families may co-opt in distinct regulatory pathways in response to IAV infection, related to Figure 5

(A) Distribution and TE peak regions on reduced families. The inset barplot shows the proportion of instances in each TE peak region. The locations and proportions (%) of the top-five TE peaks regions along the consensus sequence are shown. The number in each dot refers to the proportion (above 10%) among accessible instances in each TE peak region. It shows that most instances with reduced accessibility (in Region 1) from L1MA families are consistently located at similar locations of the 3'end of consensus sequence. Y-axis shows the family name and the number of accessible instances mapped to the top consensus sequence. TE peak regions were detected as we described in Methods. **(B)** TF binding motifs enriched in reduced families. Same motifs enriched across TE peak regions were aggregated and the proportions of instances containing each motif are shown. TE peak regions with more accessible instances are shown as representatives. Black boxes highlighted the SPI and MEF2 related motifs (green color) enriched in reduced families. It shows that Region 1s (located at around 300 bp, **Figure S6B**) of L1MA families are consistently enriched for MEF2 related motifs. MEF2 related TFs were previously reported to regulate anti-microbial genes.[5] **(C)** TFs potentially bound to different categories of families are involved in distinct pathways. Apart from AP-2 related pathways, TFs bound to high variable families are mainly involved in transcription-related pathways. TFs bound to low variable families and reduced families are mainly involved in cytokine signaling and other immune-related pathways. Bars in different colors represent different categories of families they are enriched. * indicates motifs that are enriched in different categories of families. IRF1 motif is

enriched in both low variable families and reduced families. ELF1/3 motifs are enriched in both high variable families and reduced families.

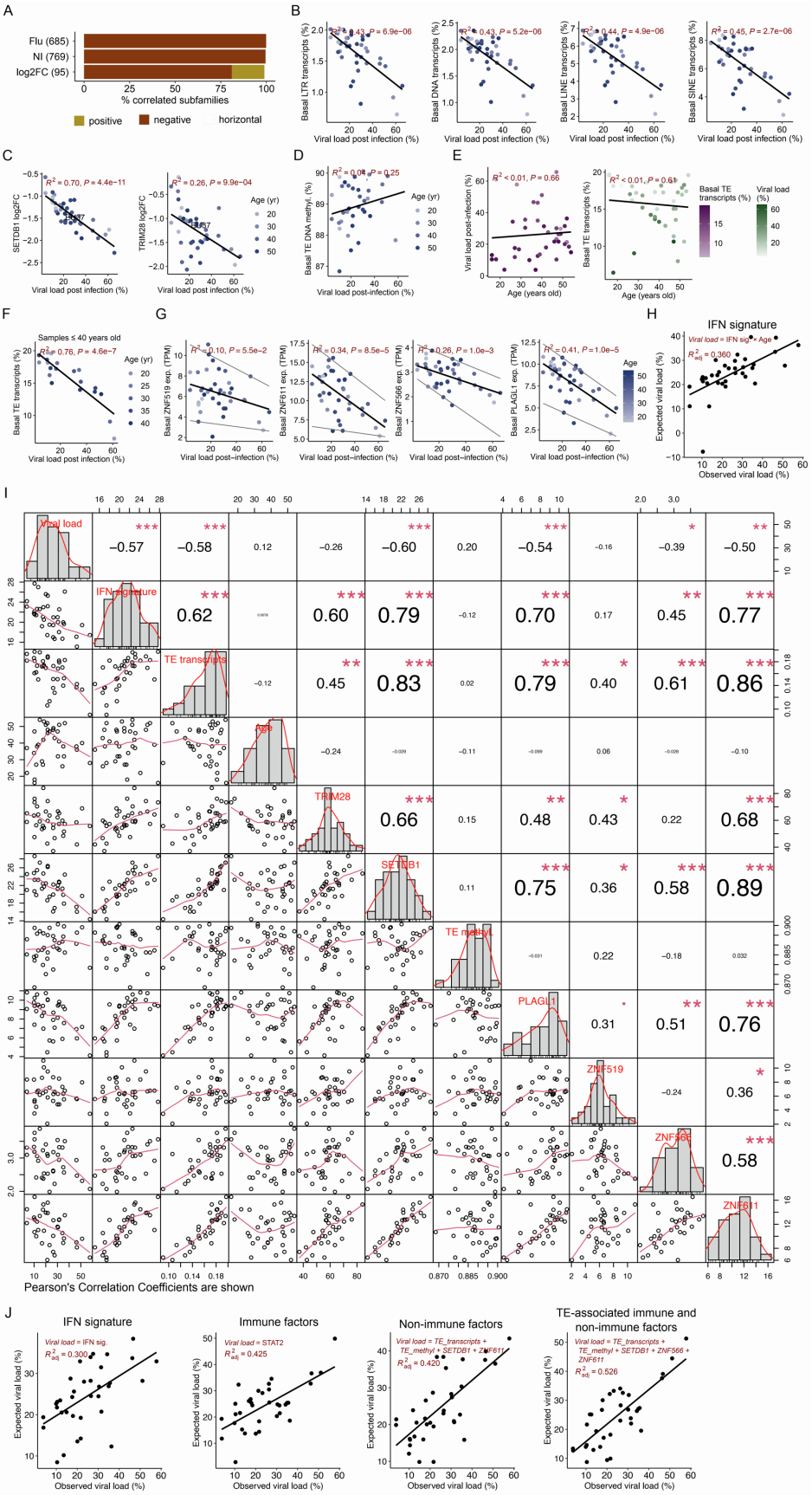
A
Flu (685)
NI (769)
log2FC (95)
% correlated subfamilies
positive
negative
horizontal
B
Basal LTR transcripts (%)
Basal DNA transcripts (%)
Basal LINE transcripts (%)
Basal SINE transcripts (%)
Viral load post infection (%)
C
SETDB1 log2FC
TRIM28 log2FC
Age (yr)
D
Basal TE DNA methyl. (%)
E
Viral load post-infection (%)
Basal TE transcripts (%)
Age (years old)
F
Samples ≤ 40 years old
G
Basal ZNF519 exp. (TPM)
Basal ZNF611 exp. (TPM)
Basal ZNF566 exp. (TPM)
Basal PLAGL1 exp. (TPM)
H
IFN signature
Expected viral load (%)
Observed viral load (%)
I
Viral load
IFN signature
TE transcripts
Age
TRIM28
SETDB1
TE methyl.
PLAGL1
ZNF519
ZNF566
ZNF611
Pearson's Correlation Coefficients are shown
J
IFN signature
Immune factors
Non-immune factors
TE-associated immune and non-immune factors

Figure S9. Correlations between TE-associated host factors and viral load post-infection, related to Figure 6

(A) Correlation directions among TE families that are correlated ($R^2 \geq 0.3$ and p value ≤ 0.05) with viral load post-infection (**Figure 6A**). More details were described in Methods. **(B)** Consistent inverse correlations between the basal transcripts of four main TE subclasses and viral load, including LTR, DNA, LINE, and SINE. The basal amount of transcript refers to the proportion of aggregated normalized read counts in each subclass among the global transcripts. Black line represents the regression line. R^2 and p values computed by the linear regression model are shown. **(C)** Correlations between the expression fold changes (log2FCs) of both *SETDB1* (left) and *TRIM28* (right) and viral load. *SETDB1* rather than *TRIM28* is shown to be inversely correlated with viral load. **(D)** Correlation between the basal DNA methylation level in TEs and viral load. Individuals with low viral load are likely to have lower TE DNA methylation levels. **(E)** Correlations between both viral load post-infection (left) and basal TE transcripts (right) and ages. Samples from younger individuals have a relatively higher amount of basal TE transcripts with a smaller deviation compared to older samples in macrophages. Two samples were identified as outliers having among the lowest amount of basal TE transcripts; strikingly, they also preserved among the highest viral load. **(F)** Correlation between the basal TE transcripts and viral load for individuals 40 years old or younger. It shows an increased correlation compared to the correlation among 39 samples (**Figure 6B**). **(G)** Correlations between the basal expression of candidate host factors and viral load post-infection. Basal *ZNF519*, *ZNF566*, *ZNF611* and *PLAGL1* expressions are both inversely correlated with viral load post-infection. **(H)** Multivariable regression model developed for the predictive of viral load post-infection using type I interferon (IFN) signature and age only. Details were described in

Methods. **(I)** Correlation matrix chart of viral load and variables that are potentially associated with IAV infection and TEs. Histograms and kernel density overlays of each variable are shown. Scatterplot matrix and absolute correlations between each of two variables and viral load are also shown. Red lines represent the distribution. R *chart.Correlation* function was used for the analysis. Pearson's correlation coefficients are shown (* $p \leq 0.05$, ** $p \leq 0.01$, *** $p \leq 0.001$). **(J)** Multivariable regression models developed for the predictive of viral load post-infection while age was included as an independent variable. We used the same sets of variables for the models included in **Figure S9H** and **Figure 6H-J**. The adjusted R^2 is significantly lower than the model developed by the inclusion of age as an interaction term variable. Details were described in Methods.

REFERENCES

1. Srinivasachar Badarinarayan, S., Shcherbakova, I., Langer, S., Koepke, L., Preising, A., Hotter, D., Kirchhoff, F., Sparrer, K.M.J., Schotta, G., and Sauter, D. (2020). HIV-1 infection activates endogenous retroviral promoters regulating antiviral gene expression. Nucleic Acids Research *48*, 10890–10908. 10.1093/nar/gkaa832.

2. Chuong, E.B., Elde, N.C., and Feschotte, C. (2016). Regulatory evolution of innate immunity through co-option of endogenous retroviruses. Science *351*, 1083–1087. 10.1126/science.aad5497.

3. Imbeault, M., Helleboid, P.-Y., and Trono, D. (2017). KRAB zinc-finger proteins contribute to the evolution of gene regulatory networks. Nature *543*, 550–554. 10.1038/nature21683.

4. Barazandeh, M., Lambert, S.A., Albu, M., and Hughes, T.R. (2018). Comparison of ChIP-Seq Data and a Reference Motif Set for Human KRAB C2H2 Zinc Finger Proteins. G3 Genes|Genomes|Genetics *8*, 219–229. 10.1534/g3.117.300296.

5. Clark, R.I., Tan, S.W.S., Péan, C.B., Roostalu, U., Vivancos, V., Bronda, K., Pilátová, M., Fu, J., Walker, D.W., Berdeaux, R., et al. (2013). MEF2 Is an In Vivo Immune-Metabolic Switch. Cell *155*, 435–447. 10.1016/j.cell.2013.09.007.